BCSJ

Sequential Structural Control of Open-Framework Nanoparticles Both in Dispersion and in Film for Electrochemical Performance Tuning

Kyoung-Moo Lee,[1,2] Akira Takahashi,[1] Hisashi Tanaka,[1] Kyung Ho Kim,[2] Midori Kawamura,[2] Yoshio Abe,[2] Manabu Ishizaki,[3] Masato Kurihara,[3] and Tohru Kawamoto*[1]

[1]Nanomaterials Research Institute, National Institute of Advanced Industrial Science and Technology (AIST), 1-1-1 Higashi, Tsukuba, Ibaraki 305-8565

[2]Department of Materials Science and Engineering, Kitami Institute of Technology, Kitami, Hokkaido 090-8507

[3]Department of Material and Biological Chemistry, Faculty of Science, Yamagata University, 1-4-12 Kojirakawa-machi, Yamagata 990-8560

E-mail: tohru.kawamoto@aist.go.jp

Received: June 10, 2015; Accepted: July 27, 2015; Web Released: November 15, 2015

Tohru Kawamoto

Dr. Tohru Kawamoto received his Ph.D. from Osaka University, Japan in 1997. From 1997 to 2001, he worked in Electrotechnical Laboratory. Since 2001, he belongs to National Institute of Advanced Industrial Science and Technology (AIST), due to the reconstruction of the organization. By 2005, he have mainly been devoting to the theoretical research for phase transition induced by external stimuli. Since 2006, the main theme has been switched to the experimental research with the nanoparticles of porous coordination polymer for the electrochromism, radioactive cesium decontamination, and other treatment of wastewater.

Abstract

We demonstrated that the sequential structural control of nanoparticles of an open-framework coordination polymer, copper hexacyanoferrate (CuHCF). The structural control has been achieved by adding the component ions not only in dispersion phase but also in the thin film form. The CuHCF nanoparticles (NPs) in the dispersion phase changed chemical composition and enhanced dispersibility with capturing $[Fe(CN)_6]^{3-}$ anions. On the other hand, the NPs in the thin film were reversibly turned to the original state by capturing Cu^{2+} cations. Through the sequential processes, all of the synthesized CuHCF NPs were utilized for the high-quality electrochemical electrode for without electrochemical side reaction. This process will contribute the preparation of various electrochemical devices such as electrochromic devices, secondary batteries and biosensors.

Recently porous materials,[1–4] especially open-framework coordination polymers, such as metal–organic frameworks[5,6] and Prussian blue analogues, have become quite attractive with their nanocavity network in the crystal. One important potential application is utilization as electrochemical electrodes, for which Prussian blue and its analogues have been investigated by various researchers especially.[7,8] The Prussian blue family, also called metal hexacyanoferrates (MHCFs), have general chemical formula $AM_x[M'(CN)_6]_y$, where A represents the cation such as alkali metals, and M and M′ are metals with various oxidation numbers.[7,9–14] The MHCFs are low cost materials synthesized with simple processes, often exhibiting an excellent electrochemical reaction with long cycle stability and fast response, where the nanocavity network is utilized for fast and stable ion diffusion.[15–19]

In addition, solvent-dispersible MHCF nanoparticles have received attention in recent years, because of the importance of fabricating thin films and fine patterns for printed electronics.[16,20–25] The dispersibility of the MHCF nanoparticles are improved by a simple method:[23,24] Synthesis of the insoluble nanoparticles of the MHCF with mixing $M^{\alpha+}$ cations and $[Fe(CN)_6]^{\beta-}$ anions, followed by the addition of chemicals for surface modification. By changing the added chemicals, the dispersibility for various solvents such as water, alcohols, and organic solvents is provided.

In this paper, we further developed the method: realizing the water-dispersibility control, both enhancement in the aqueous dispersion and suppression in the thin film. As an example, we used copper hexacyanoferrate (CuHCF), also a fascinating material with various potential applications,[26–41] especially for electrochemical applications such as secondary battery electrodes,[26,27] electrochromic devices,[28,29] and chemical sensors.[30–33]

The essential strategy is schematically shown in Figure 1. First, the insoluble CuHCF nanoparticles are given water-dispersibility by adding $[Fe(CN)_6]^{\beta-}$ anions in a suspension liquid (slurry), by raising the polarizability of nanoparticles negatively by capturing the anions (called CuHCF(−) in this paper). Sequentially, the dispersibility is reversely suppressed by capturing the Cu^{2+} cation even after fabricating the thin film

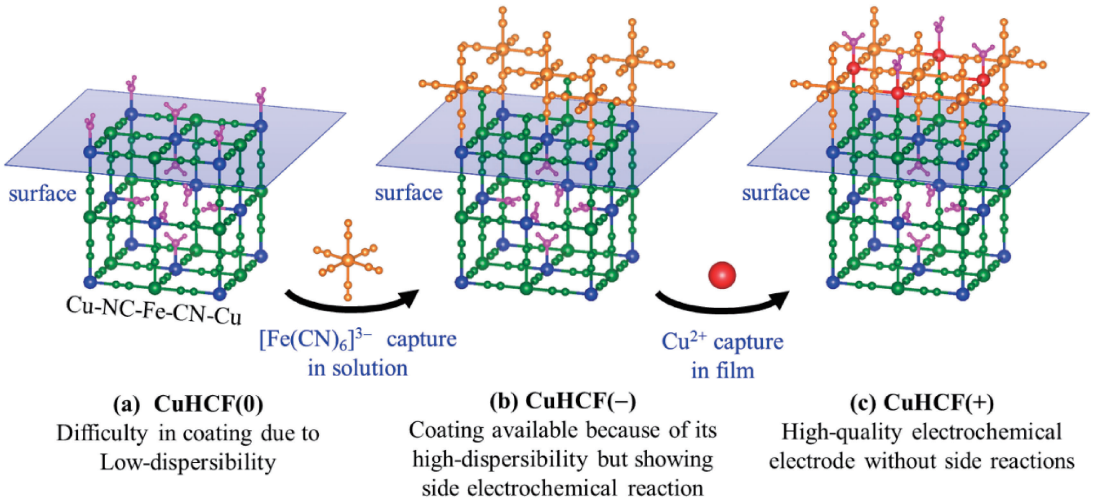

Figure 1. A schematic view of the sequential structural control of CuHCF. These blocks show the surface crystal structure of CuHCF nanoparticle. The blue, green, and violet units respectively represent Cu^{2+}, $[Fe(CN)_6]^{3-}$, and H_2O originally included in CuHCF(0). The orange and red units show the additive $[Fe(CN)_6]^{3-}$ and Cu^{2+}, respectively.

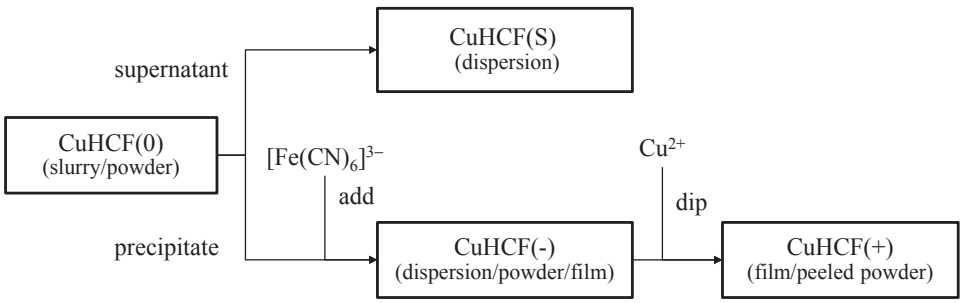

Figure 2. Schemes of the preparation method of the CuHCF nanoparticles and their obtained form.

(called CuHCF(+)). The most important point is both captured ions, the raw materials of the MHCF, indicating that they would not obstruct the electrochemical reactions of the CuHCF. Another specialty of our method is the suppression of the dispersibility even in thin film without heating. The dispersibility of nanoparticles is disadvantages for the thin-film stability, although it is required in the coating/printing processes for the film fabrication. In addition, the film-immobilization by heating is often difficult to apply due to the limitation of the heat stability of the substrate.

To realize our strategy shown in Figure 1, we determined the amount of the added ions, e.g. in the case of the preparation of CuHCF(−), we used slightly more of the additional $[Fe(CN)_6]^{\beta-}$ anions than the Cu-site on the CuHCF(0) surfaces for the sufficient coverage of the nanoparticle surface. However, we do not deny the occurrence of the insertions of the anions and cations into the NPs. Even with the ion insertions into NPs, our purpose, the control of the dispersibility and the electrochemical reaction, would be achieved wherever the positions of the added ions captured in the NPs.

Our method also provides further improvement: the elimination of electrochemical side-reactions of the nanoparticle electrode. The MHCF thin films often show a side redox reaction, mainly caused by excessive raw materials. Such side reaction disappears with our method, which leads to the stable work in electrochemical devices.

In this paper, we elucidate the structural change during the ion-capture processes, e.g. chemical composition, crystal structure, and the nanoparticle form. The tuning of the electrochemical performance is also clarified, especially colour variation in the electrochromism, the optical property change by the redox reactions.

Experimental

Four kinds of CuHCF were prepared in this study. The preparation scheme and their form is summarized in Figure 2.

At first, we prepared as-synthesized CuHCF (CuHCF(0)) nanoparticles according to previous reports.[23,29] The CuHCF(0) nanoparticles were synthesized by mixing two raw material solutions in a Y-type micromixer with a hole diameter of 150 μm.[42] The concentrations of solutions were adjusted to 0.6 mol L^{-1} of $CuSO_4$ and 0.4 mol L^{-1} of $K_3[Fe(CN)_6]$. The CuHCF(0) with a chemical composition of $Cu^{II}[Fe^{III}(CN)_6]_{2/3}\cdot zH_2O$ was synthesized by the following reaction:

$$CuSO_4 + 2/3K_3[Fe(CN)_6] \rightarrow Cu^{II}[Fe^{III}(CN)_6]_{2/3} + K_2SO_4 \quad (1)$$

The flow rates of the two solutions were equal (each 50 mL min^{-1}) and the total of them was adjusted to 100 mL min^{-1}. The size of CuHCF(0) nanoparticles are expected to ca. 20 nm. The obtained CuHCF(0) slurry was washed with Milli-Q water four times by centrifugation to remove K_2SO_4. Because of the

difficulty of the homogeneous thin film fabrication with CuHCF(0) due to their low dispersibility, we also used the supernatant, CuHCF(S), in order to fabricate the CuHCF(0) thin films.

In order to prepare the CuHCF(−) with higher dispersibility, 0.075 mol L^{-1} $K_3[Fe(CN)_6]$ aqueous solution was added to the CuHCF(0) slurry with the molar ratio of $[Fe(CN)_6]^{3-}$/$Cu[Fe(CN)_6]_{2/3} = 0.25$. After stirring at room temperature over three days, the CuHCF(−) were obtained as dispersion liquid without any precipitate.

We prepared electrochemical electrodes with CuHCF(S) and with CuHCF(−) thin film. The thin film of each CuHCF sample was fabricated on an indium tin oxide (ITO)/glass substrate by spin-coating with each dispersion liquid with the concentration of 0.1 g mL^{-1}. The film thickness was controlled with the rotation rate for matching 6–9 mC cm^{-2} of the transferred charge density in redox reactions. The thickness of each thin film was confirmed as about 250–350 nm from the FE-SEM images. We also prepared cation-capturing CuHCF (CuHCF(+)) thin film, by quickly dipping in 0.1 mol L^{-1} $CuSO_4 \cdot 5H_2O$ aqueous solution, followed by a rinse with water.

The crystal structures of the CuHCF(0), CuHCF(−), and CuHCF(+) were evaluated by X-ray diffraction (XRD) at room temperature using Cu Kα ($\lambda = 1.54$ Å) radiation in the 2θ range of 10–70° (Ultima III, Rigaku, Japan). The crystallite sizes were estimated by the Scherrer analysis of the XRD patterns assuming the Scherrer constant = 0.94.[43] The CuHCF(−) and CuHCF(0) were evaluated with their powders. Only for CuHCF(+), thin film was used.

For the evaluation of the dispersibility of CuHCF(S), CuHCF(−), and CuHCF(+), the zeta potentials were measured by dynamic light scattering (DLS) measurement (Delsa™ Nano HC Particle Analyzer, Beckman Coulter, Inc., Ireland) with the sample concentration of 2.5 mg mL^{-1} with the range of pH 7–8 at 25 °C. For the CuHCF(S) and CuHCF(−), we used aqueous dispersions. But for CuHCF(+), the aqueous dispersion of the powders obtained by peeling the thin film was evaluated.

The chemical compositions of CuHCF were characterized by microwave plasma atomic emission spectrometry (MP-AES, 4100 MP-AES, Agilent Technologies, USA) with predecomposition using a microwave sample preparation system (MW, Multiwave3000, Perkin-Elmer Corp., USA). The surface morphology and the structure of the CuHCF thin films were evaluated using a field emission scanning electron microscope (FE-SEM, S-4800II, Hitachi Ltd., Japan).

The electrochemical and electrochromic properties of the thin film electrode of CuHCF(S), CuHCF(−), and CuHCF(+) were measured using cyclic voltammetry (CV) with a potentiostat (ALS600E, BAS, Japan). In situ optoelectrochemical measurements were carried out with a UV–vis spectrometer (USB-4000; Ocean Optics Inc.). For the reference electrode, the counter one, and the electrolyte, we used a saturated calomel electrode (SCE), platinum wire, and 0.1 mol L^{-1} potassium bis(trifluoromethanesulfonyl)imide (KTFSI)/propylene carbonate (PC) solution, respectively.

Results and Discussion

Compositions. The chemical composition of CuHCF also indicates the sequential structural control of nanoparticles. Table 1 shows the chemical compositions of each CuHCF. It is found that the composition ratio of Fe to Cu (Fe/Cu) increased in CuHCF(−) and decreased in CuHCF(+), respectively, indicating that the capture of $[Fe(CN)_6]^{3-}$ anion and Cu^{2+} cation by NPs were achieved in each sequential step. On the other hand, in the case of CuHCF(+) preparation with additive Cu^{2+}, the chemical composition almost returned to that of the CuHCF(0), indicating that the most stable composition would be Fe/Cu = 2/3.

The changes of the Fe/Cu ratio are reasonable with the concept shown in Figure 1, e.g. In the case of the CuHCF(−) preparation with the additive $[Fe(CN)_6]^{3-}$, Fe/Cu increased to 31%. When the CuHCF(0) is assumed to be a cubic shape with their NPs size 10–20 nm, the Cu^{2+} site on the NPs-surface, that would capture the additive $[Fe(CN)_6]^{3-}$ by coordination bonding, is 14–27% of all Cu^{2+} ions. The excess $[Fe(CN)_6]^{3-}$ anions would remain as $K_3[Fe(CN)_6]$.

Crystal Structure. From the crystal structure analysis, we observed a behavior of the excess $[Fe(CN)_6]^{3-}$ anions, added into the CuHCF(0) at the process of the preparation of the CuHCF(−). With XRD spectra shown in Figure 3, we found the existence of excess $[Fe(CN)_6]^{3-}$ anions as $K_3[Fe(CN)_6]$ in CuHCF(−), and their disappearance in CuHCF(+).

Zeta Potentials. The zeta potentials of CuHCF were evaluated as shown in Table 2. Generally the dispersibility of nanoparticles increased as their zeta potential increased, implying that the order of the dispersibility is CuHCF(−), CuHCF(S), and CuHCF(+). It is consistent with our strategy as shown in Figure 1. In CuHCF(−), after $[Fe(CN)_6]^{3-}$ anions are added into CuHCF(0), zeta-potential is negatively increased,

Table 1. Compositions of CuHCF samples measured by MP-AES

Nanoparticles	Compositions	Fe/Cu	Δ(Fe/Cu)
CuHCF(0)	$K_{0.05}Cu[Fe(CN)_6]_{0.68}$	0.68	—
CuHCF(−)	$K_{1.00}Cu[Fe(CN)_6]_{0.99}$	0.99	0.31
CuHCF(+)	$K_{0.01}Cu[Fe(CN)_6]_{0.71}$	0.71	−0.28

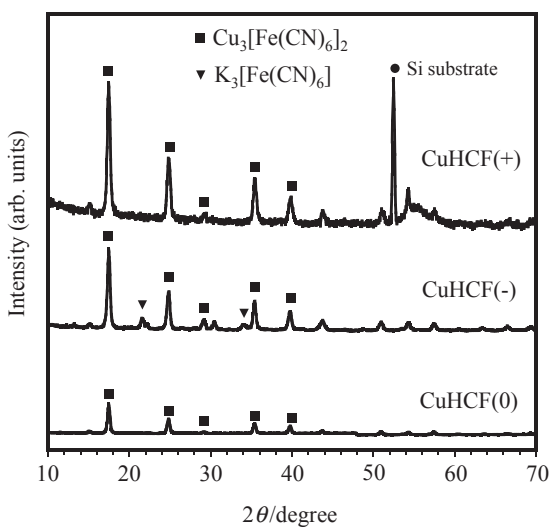

Figure 3. XRD patterns of CuHCF(0), CuHCF(−), and CuHCF(+).

Table 2. Zeta potentials of CuHCF nanoparticles

Nanoparticles	Zeta potential/mV
CuHCF(S)	−39.70
CuHCF(−)	−46.56
CuHCF(+)	−27.48

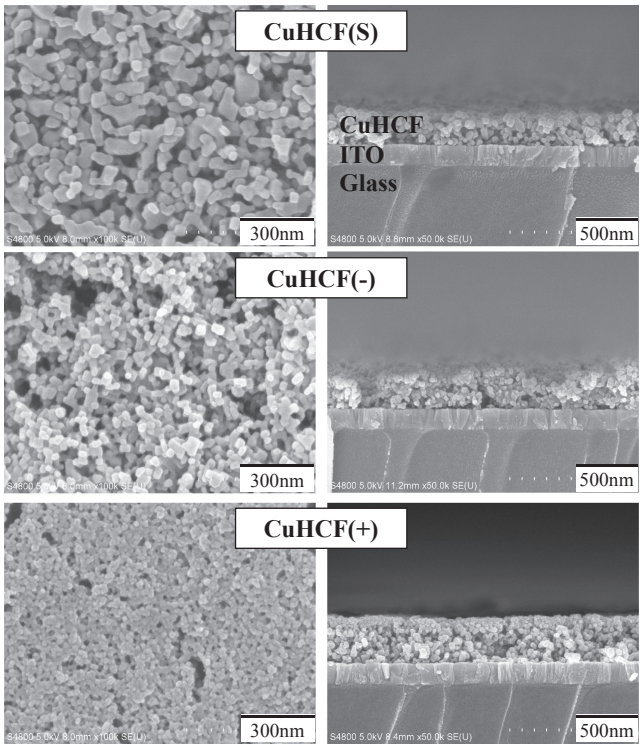

Figure 4. FE-SEM images of CuHCF thin films. Left: surface, right: cross-section.

indicating successful capture of $[Fe(CN)_6]^{3-}$ anions by the CuHCF(0). On the other hand, when Cu^{2+} cation is introduced to CuHCF(−) to prepare the CuHCF(+), the absolute value of the zeta potential becomes small (close to "0"), showing that the Cu^{2+} ions are captured by CuHCF(−). Because CuHCF(S) is just the supernatant of CuHCF(0), CuHCF(S) would be the part of CuHCF(0) having larger zeta potential accidentally.

The CuHCF(+) electrode is stable even in water, although the CuHCF(−) electrode easily eluted in contacting with water. This result shows that the dispersibility of nanoparticles and the electrode stability against the water contact is controlled by Cu^{2+} ion-capturing.

Morphology. The influence on the morphology of the CuHCF thin film by the sequential ion-capture processes is found in the FE-SEM images shown in Figure 4. Concerning the effect of the additive $[Fe(CN)_6]^{3-}$ ions, between CuHCF(S) and CuHCF(−), the size of nanoparticles seems smaller in CuHCF(−) than in CuHCF(S). Such downsizing of the nanoparticles is caused by the enhancing of repulsion among primary nanoparticles. In contrast, the change of the size of nanoparticles through the Cu^{2+}-capture between CuHCF(−) and CuHCF(+) is interesting. The CuHCF(+) film seems to form a two layered structure with the upper smaller nanoparticles and the lower

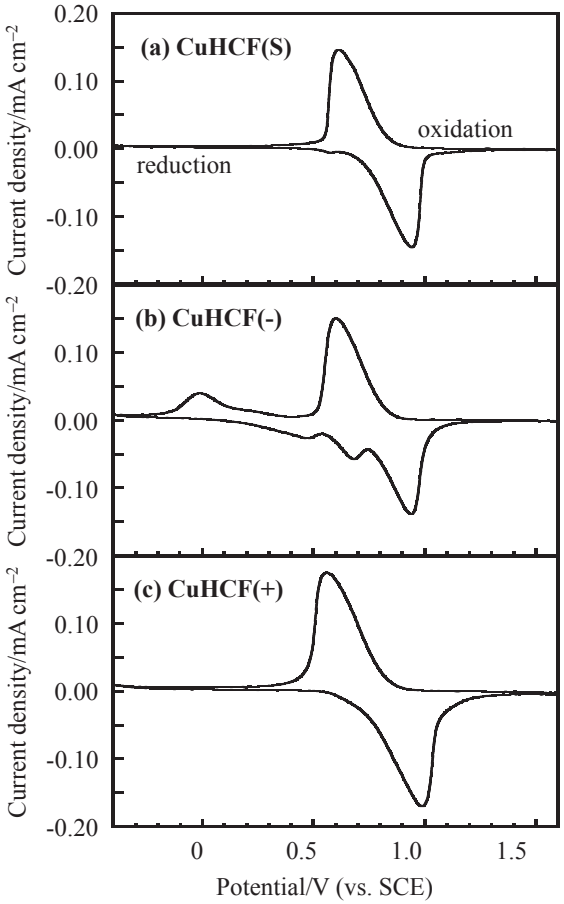

Figure 5. Cyclic voltammogram of each CuHCF film electrodes (Scan rate: 5 mV s^{-1}).

larger ones. The upper layer of CuHCF(+) thin film would be the new CuHCF formation from the excess $[Fe(CN)_6]^{3-}$ anions in the anion-capture process and the additive Cu^{2+} in the cation-capture one.

Electrochemical Properties. In electrochemical properties, the effects of the anion/cation capture were clearly found. Concerning with CuHCF(S), supernatant of CuHCF(0), the clear electrochemical reaction was observed. The cyclic voltammograms of CuHCF films electrode are shown in Figure 5. The main peaks reveal redox reaction between Fe^{2+} and Fe^{3+} as the following eq 2:

$$Cu^{II}{}_3[Fe^{III}(CN)_6]_2 + 2K^+ + 2e^- \rightleftharpoons K_2Cu^{II}{}_3[Fe^{II}(CN)_6]_2 \quad (2)$$

On the other hand, the CuHCF(S) and CuHCF(−) electrode have satellite peaks corresponding to the side reaction. Especially the CuHCF(−) electrode shows large side reactions. The side reaction in CuHCF(−) would correspond to the redox reaction of the excess $[Fe(CN)_6]^{3-}$, because the side reactions were enhanced in CuHCF(−) after addition of the $[Fe(CN)_6]^{3-}$. The side reaction is suppressed by Cu^{2+} capture as shown in CuHCF(+), caused by disappearance of the $[Fe(CN)_6]^{3-}$ with the new CuHCF formation. The important point is that no difference is found in the cyclic voltammogram between CuHCF(S) and CuHCF(+). This result indicates that our method with sequential structural control supplies CuHCF

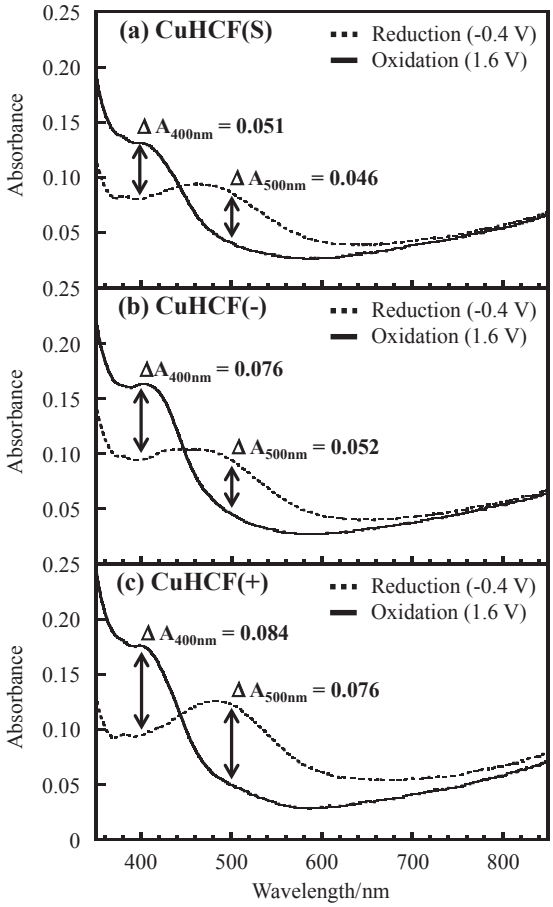

Figure 6. Absorbance spectra of CuHCF film electrodes by redox reaction. The spectra for reduction and oxidation states were measured after applying the potential at −0.4 and 1.6 V vs. SCE for 200 s, respectively.

Table 3. Absorbance change of CuHCF films by $[Fe(CN)_6]^{3-}$ and Cu^{2+} ion-capturing

Thin film electrodes	ΔA_{400nm}		ΔA_{500nm}	
CuHCF(S)	0.051	—	0.046	—
CuHCF(−)	0.076	49%[a)]	0.052	13%[a)]
CuHCF(+)	0.084	11%[b)]	0.076	46%[b)]

a) Increased absorbance percentage by $[Fe(CN)_6]^{3-}$-capturing.
b) Increased absorbance percentage by Cu^{2+}-capturing.

thin film exhibiting high-quality electrochemical reactions, and with high yield. Because the CuHCF(S) were just supernatant, we can use only the small part of CuHCF(0) for thin film preparation. Besides by the sequential structural control, all of the synthesized CuHCF can be utilized for the thin film.

Electrochromic Properties. Finally we demonstrated the electrochromic properties of all the CuHCF films. The oxidized and reduced states of the CuHCF films show absorbance peak around 400 and 500 nm, respectively as shown in Figure 6. The changes of these absorbance peak changes, shown in Table 3, correspond to the variation of the chemical composition. The ratio $\Delta A_{400nm}/\Delta A_{500nm}$ is almost the same between CuHCF(S) and CuHCF(+), indicating that the sequential structural control well reproduced the initial electrochromic properties.

Conclusion

In conclusion, we demonstrated the sequential structural control of the open-framework Prussian blue-type nanoparticles, CuHCF, by the ion-capture processes both in the dispersion phase and in the thin film. The Fe/Cu ratio in the chemical composition can reversibly be varied between 0.68 and 0.99, providing control of the dispersibility. The process also results in excellent electrochemical reactions without any side reactions. This approach will contribute to the preparation of electrochemical electrodes of open-framework nanoparticles for secondary batteries, electrochromic devices and biosensors.

Some data of this work were obtained utilizing the Nano-Processing Facility, supported by IBEC Innovation platform, AIST.

References

1 K. Ariga, Y. Yamauchi, G. Rydzek, Q. Ji, Y. Yonamine, K. C.-W. Wu, J. P. Hill, *Chem. Lett.* **2014**, *43*, 36.
2 B. P. Bastakoti, S. Ishihara, S.-Y. Leo, K. Ariga, K. C.-W. Wu, Y. Yamauchi, *Langmuir* **2014**, *30*, 651.
3 K. Ariga, A. Vinu, Y. Yamauchi, Q. Ji, J. P. Hill, *Bull. Chem. Soc. Jpn.* **2012**, *85*, 1.
4 Y.-H. Yang, C.-H. Liu, Y.-H. Liang, F.-H. Lin, K. C.-W. Wu, *J. Mater. Chem. B* **2013**, *1*, 2447.
5 S. Kitagawa, R. Kitaura, S. Noro, *Angew. Chem., Int. Ed. Engl.* **2004**, *43*, 2334.
6 F.-K. Shieh, S.-C. Wang, S.-Y. Leo, K. C.-W. Wu, *Chem.—Eur. J.* **2013**, *19*, 11139.
7 N. R. de Tacconi, K. Rajeshwar, R. O. Lezna, *Chem. Mater.* **2003**, *15*, 3046.
8 A. A. Karyakin, *Electroanalysis* **2001**, *13*, 813.
9 K. Itaya, I. Uchida, V. D. Neff, *Acc. Chem. Res.* **1986**, *19*, 162.
10 H. Tokoro, T. Matsuda, T. Nuida, Y. Moritomo, K. Ohoyama, E. D. L. Dangui, K. Boukheddaden, S. Ohkoshi, *Chem. Mater.* **2008**, *20*, 423.
11 S. Ohkoshi, K. Hashimoto, *J. Am. Chem. Soc.* **1999**, *121*, 10591.
12 O. Sato, T. Iyoda, A. Fujishima, K. Hashimoto, *Science* **1996**, *271*, 49.
13 V. Escax, A. Bleuzen, C. Cartier dit Moulin, F. Villain, A. Goujon, F. Varret, M. Verdaguer, *J. Am. Chem. Soc.* **2001**, *123*, 12536.
14 Y. Einaga, *Bull. Chem. Soc. Jpn.* **2006**, *79*, 361.
15 K. Itaya, *J. Appl. Phys.* **1982**, *53*, 804.
16 S. Hara, H. Shiozaki, A. Omura, H. Tanaka, T. Kawamoto, M. Tokumoto, M. Yamada, A. Gotoh, M. Kurihara, M. Sakamoto, *Appl. Phys. Express* **2008**, *1*, 104002.
17 K. Moo Lee, H. Tanaka, K. Ho Kim, M. Kawamura, Y. Abe, T. Kawamoto, *Appl. Phys. Lett.* **2013**, *102*, 141901.
18 K.-M. Lee, H. Tanaka, A. Takahashi, K. H. Kim, M. Kawamura, Y. Abe, T. Kawamoto, *Electrochim. Acta* **2015**, *163*, 288.
19 T. Shibata, Y. Moritomo, *Chem. Commun.* **2014**, *50*, 12941.
20 D. M. DeLongchamp, P. T. Hammond, *Chem. Mater.* **2004**, *16*, 4799.
21 M. Yamada, M. Arai, M. Kurihara, M. Sakamoto, M. Miyake, *J. Am. Chem. Soc.* **2004**, *126*, 9482.

22 T. Uemura, S. Kitagawa, *Chem. Lett.* **2005**, *34*, 132.
23 A. Gotoh, H. Uchida, M. Ishizaki, T. Satoh, S. Kaga, S. Okamoto, M. Ohta, M. Sakamoto, T. Kawamoto, H. Tanaka, M. Tokumoto, S. Hara, H. Shiozaki, M. Yamada, M. Miyake, M. Kurihara, *Nanotechnology* **2007**, *18*, 345609.
24 M. Ishizaki, K. Kanaizuka, M. Abe, Y. Hoshi, M. Sakamoto, T. Kawamoto, H. Tanaka, M. Kurihara, *Green Chem.* **2012**, *14*, 1537.
25 S. Hara, H. Tanaka, T. Kawamoto, M. Tokumoto, M. Yamada, A. Gotoh, H. Uchida, M. Kurihara, M. Sakamoto, *Jpn. J. Appl. Phys.* **2007**, *46*, L945.
26 M. Pasta, C. D. Wessells, N. Liu, J. Nelson, M. T. McDowell, R. A. Huggins, M. F. Toney, Y. Cui, *Nat. Commun.* **2014**, *5*, 3007.
27 M. Jayalakshmi, F. Scholz, *J. Power Sources* **2000**, *91*, 217.
28 A. P. Baioni, M. Vidotti, P. A. Fiorito, E. A. Ponzio, S. I. C. De Torresi, *Langmuir* **2007**, *23*, 6796.
29 M. Ishizaki, M. Sakamoto, H. Tanaka, T. Kawamoto, M. Kurihara, *Mol. Cryst. Liq. Cryst.* **2011**, *539*, 18/[358].
30 R. Garjonyte, A. Malinauskas, *Sens. Actuators, B* **1999**, *56*, 93.
31 T.-H. Tsai, T.-W. Chen, S.-M. Chen, K.-C. Lin, *Int. J. Electrochem. Sci.* **2011**, *6*, 2058.
32 T.-H. Tsai, T.-W. Chen, S.-M. Chen, *Int. J. Electrochem. Sci.* **2011**, *6*, 4628.
33 L. Guadagnini, D. Tonelli, M. Giorgetti, *Electrochim. Acta* **2010**, *55*, 5036.
34 M. Avila, L. Reguera, J. Rodríguez-Hernández, J. Balmaseda, E. Reguera, *J. Solid State Chem.* **2008**, *181*, 2899.
35 C. P. Krap, J. Balmaseda, L. F. del Castillo, B. Zamora, E. Reguera, *Energy Fuels* **2010**, *24*, 581.
36 S. Ayrault, B. Jimenez, E. Garnier, M. Fedoroff, D. Loos-Neskovic, *J. Solid State Chem.* **1998**, *141*, 475.
37 C. Loos-Neskovic, S. Ayrault, V. Badillo, B. Jimenez, E. Garnier, M. Fedoroff, D. J. Jones, B. Merinov, *J. Solid State Chem.* **2004**, *177*, 1817.
38 R. Chen, H. Tanaka, T. Kawamoto, M. Asai, C. Fukushima, M. Kurihara, M. Ishizaki, M. Watanabe, M. Arisaka, T. Nankawa, *ACS Appl. Mater. Interfaces* **2013**, *5*, 12984.
39 R. Chen, H. Tanaka, T. Kawamoto, M. Asai, C. Fukushima, M. Kurihara, M. Watanabe, M. Arisaka, T. Nankawa, *Electrochem. Commun.* **2012**, *25*, 23.
40 C. P. Krap, J. Balmaseda, B. Zamora, E. Reguera, *Int. J. Hydrogen Energy* **2010**, *35*, 10381.
41 G. B. Barton, J. L. Hepworth, E. D. McClanahan, R. L. Moore, H. H. Van Tuyl, *Ind. Eng. Chem.* **1958**, *50*, 212.
42 A. Takahashi, N. Minami, H. Tanaka, K. Sue, K. Minami, D. Parajuli, K.-M. Lee, S. Ohkoshi, M. Kurihara, T. Kawamoto, *Green Chem.* **2015**, *17*, 98.
43 P. Scherrer, *Nachr. Ges. Wiss. Göttingen* **1918**, *26*, 98.